Research Square

Preprints are preliminary reports that have not undergone peer review.
They should not be considered conclusive, used to inform clinical practice,
or referenced by the media as validated information.

In vitro effects of low-molecular-weight organic acids on phosphorus transcriptional response in bacterial strains

Carol Jerez-Quezada
Michel Abanto
Patricio Barra
Daniel Menezes-Blackburn
María de la Luz Mora
mariluz.mora@ufrontera.cl

Universidad de La Frontera https://orcid.org/0000-0002-7474-1595

Research Article

Keywords: Phosphate acquisition, Organic acids, pstS, phoE, phoA, Volcanic soils

Posted Date: September 23rd, 2026

DOI: https://doi.org/10.21203/rs.3.rs-10897287/v1

License: This work is licensed under a Creative Commons Attribution 4.0 International License. Read Full License

Abstract

Background and aims

Low-molecular-weight organic acids (LMWOAs) are major components of plant root exudates that contribute to phosphorus (P) mobilization and influence rhizosphere microbial communities. However, their relationships with phosphate-solubilizing microorganisms and P-related functional genes have been examined in complex soil–plant systems, making it difficult to distinguish specific influence of individual LMWOAs. This study aimed to examine their influence on P-acquisition responses of phosphate-solubilizing bacteria (PSB).

Methods

Three PSB strains from volcanic Andisols of southern Chile (*Klebsiella michiganensis* RC3 and RCJ4, and *Enterobacter ludwigii* RJAL6_2) were exposed to citric, malic, and oxalic acids under controlled conditions based on a simplified experimental model. Bacterial growth, soluble P, and transcriptional responses were analyzed with comparative genomic analyses.

Results

Comparative genomic analyses revealed conserved repertoires of genes involved in P-acquisition and LMWOAs metabolism across the three strains. RC3 and RCJ4 shows an optimal growth in all LMWOAs tested, whereas RJAL6_2 showed optimal growth in citric and malic acids, but decrease when it growths in oxalic acid. Despite the low growth of RJAL6_2 on oxalic acid, this strain displayed coordinate overexpression of *phoA, phoE*, and *pstS* genes.

Conclusion

The model distinguished the influence of bacterial P-acquisition responses by reducing rhizosphere complexity and evaluating individual LMWOAs. Conserved genomic repertoires indicate that physiological and transcriptional responses were not coupled. In this sense, the findings highlight that bacterial growth responses to root metabolites. It also suggested an additional regulatory process that may influence microbial P acquisition and rhizosphere P cycling.

Introduction

As a result of high population growth, food demand is increasing, making it of utmost importance to promote sustainable and efficient agronomic nutrient use (Koul et al., 2022). In Chile, agriculture is a key driver of employment and exports (ODEPA, 2022, 2024), but its productivity depends strongly on soil nutrient status (Dai et al., 2020). Andisol soils constitute between 50% and 60% of Chile's arable soils. However, despite their high organic matter content, these soils have a low pH and low P availability due to strong sorption and precipitation with Al/Fe phases (Arifin et al., 2022; Neculman et al., 2021). P is an essential nutrient for plants, playing a central role in ATP synthesis, enzyme regulation, and photosynthesis (Assuero et al., 2004; Johan et al., 2021). Conventionally, soils are fertilized with phosphate fertilizers derived from phosphate rock (PR) (FAO, 2008); however, given population growth, PR reserves are estimated to be depleted within approximately 50–100 years (Xiong et al., 2020). Therefore, a complementary route is to use the native P of the soil, and P legacy, as well as to recycle the P of organic amendments with high amounts of total P (Barra et al., 2026; Paredes et al., 2021; Poblete-Grant et al., 2020, 2022).

Both plants and microorganisms contribute to the mobilization of P through complementary mechanisms. Microorganisms produce a set of enzymes involved in organic P mineralization and insoluble P solubilization (phosphatases, phytases, and phosphonatases), in addition to the exudation of LMWOAs, thereby releasing orthophosphates, compounds usable by plants and microorganisms alike (Boden et al., 2024; Park et al., 2022; Siles et al., 2022). Plants, in turn, exude considerably higher concentrations of LMWOAs, such as malate, citrate, and oxalate. Under acidic pH conditions, as in Andisol-type soils, these acids can exist in multiple protonation states, which influences P solubilization, by affecting the capacity of $Al^{3+,}$ Fe^{3+} and Ca^{2+} to be dissolved and chelated by protons (Rodríguez et al., 2023; Saxena et al., 2016). Although some organic acids may exhibit antimicrobial effects *in vitro* (Hirshfield et al., 2003; Kovanda et al., 2019), growing evidence indicates that in soils they play a dual role, both mobilizing P and modulating microbial activity and function in the rhizosphere (Wang, Luo, et al., 2023).

The amount and composition of LMWOA exudates are strongly influenced by environmental conditions, and these changes also affect the activity of P-mineralizing and P-solubilizing microorganisms in the rhizosphere (Mingji et al., 2009; Mora et al., 2009; Parra-Almuna et al., 2024). While the role of LMWOAs in P solubilization has been extensively documented through their ability to mobilize sparingly available P by ligand exchange, metal chelation, and mineral dissolution (Menezes-Blackburn et al., 2016, 2021; Negrón et al., 2025; Paredes et al., 2021), recent studies have shifted attention toward their potential influence on rhizosphere microorganisms (Wang, Luo, et al., 2023; Wei et al., 2018; Zheng et al., 2026). These studies suggest that changes in LMWOA availability are associated with shifts in phosphate-solubilizing microbial communities and the prevalence of P-related functional genes, indicating that LMWOAs may influence microbial P acquisition beyond their established role in P mobilization. However, because these observations have been obtained from complex soil–plant systems, they do not allow discrimination between direct transcriptional responses induced by individual LMWOAs and indirect effects resulting from changes in P availability, microbial interactions, or other metabolites present in the rhizosphere. Consequently, whether individual LMWOAs directly regulate the transcription of bacterial P acquisition genes remains unresolved.

Bacterial adaptation to P limitation involves coordinated transcriptional responses. Under P-limited conditions, many bacteria activate the Pho regulon to coordinate the expression of genes associated with the uptake, transport, and assimilation of P (Barra et al., 2023; Bruna et al., 2026; Santos-Beneit, 2015). Among these genes, *phoA* encodes an alkaline phosphatase involved in the mineralization of organic P compounds, *pstS* encodes the phosphate-binding periplasmic component of the high-affinity *Pst* transport system, and *phoE* encodes a phosphate deficiency-inducible outer membrane porin that facilitates the absorption of anionic compounds under P-limiting conditions (Oliverio et al., 2020). Although the Pho regulon is primarily activated in response to P starvation, root-derived LMWOAs may also influence these regulatory responses by modifying P availability and the physicochemical conditions surrounding bacterial cells. Therefore, it remains unclear whether these microbial responses arise from the influence of LMWOAs themselves or from other factors acting simultaneously in the soil environment. Examining isolated bacterial strains exposed to individual LMWOAs under controlled conditions provides a simplified experimental framework to elucidate the specific influence of these compounds on P acquisition gene expression and to assess whether transcriptional responses differ among phosphate-solubilizing bacterial strains.

To address these questions, we selected three native phosphate-solubilizing bacterial isolates previously recovered from the rhizosphere and endosphere of *Lolium perenne* growing in Andisols of southern Chile (Mora et al., 2017). These isolates were subsequently characterized by Barra et al. (2023), who demonstrated multiple plant growth-promoting traits, including indole-3-acetic acid production, phytate mineralization, phosphate solubilization, siderophore production, extracellular phosphatase activity, and the production of several LMWOAs. Based on these characteristics, two *Klebsiella* isolates (one rhizospheric and one endophytic) and one rhizospheric *Enterobacter* isolate were selected because of their phosphate-solubilizing capacity, extracellular phosphatase activity, and LMWOA production. Since these isolates produce the same organic acids previously reported as dominant components of *Lolium perenne* root exudates in these soils (Mora et al., 2009; Parra-Almuna et al., 2024), they provide an appropriate model for investigating bacterial responses to representative plant-derived LMWOAs.

The present study investigated native P-solubilizing bacteria isolated from Andisols in La Araucanía and evaluated how representative rhizosphere organic acids influence bacterial responses under P-limiting conditions. Specifically, the effects of malic, citric, and oxalic acids on bacterial growth were evaluated, and the expression of key genes for P acquisition, such as *phoA, phoE*, and *pstS*, was examined. In addition, comparative genomic analyses were performed to identify genes associated with P acquisition and organic acid metabolism. It was hypothesized that LMWOAs differentially regulate the expression of P acquisition genes and that these responses are strain-dependent. By integrating physiological, genomic, and transcriptional analyses, this study aimed to identify the expression patterns associated with P acquisition in bacteria adapted to acidic volcanic soils.

Materials and Methods

Phosphobacteria complete genome sequencing

We used three plant growth-promoting bacteria (PGPB) isolated from the rhizosphere and endosphere of ryegrass (*Lolium perenne*) grown in acidic volcanic Andisols of the La Araucanía Region, southern Chile (38°50' S, 72°41' W). All three were selected for established plant growth-promoting traits, including P-solubilizing capacity and acidic/alkaline phosphatase activity described by Mora et al., (2017) Barra et al., (2018, 2019, 2023) Strains RC3 and RCJ4 were sourced from the CChRGM microbial collection (Instituto de Investigaciones Agropecuarias, INIA, Chillán); strain RJAL6_2 came from the CCCT collection at the Núcleo Científico y Tecnológico BIOREN–UFRO, Temuco. Total genomic DNA was extracted from each strain using the Quick-DNA Fungal/Bacterial Miniprep Kit (Zymo Research) following the manufacturer's instructions; DNA concentration was quantified using a Qubit 4 Fluorometer (Thermo Fisher Scientific), and integrity was verified by electrophoresis on a 1% (w/v) agarose gel. The genomes of strains RC3, RCJ4, and RJAL6_2 were then sequenced on the Oxford Nanopore MinION platform using R10.4 chemistry (available in 2025). Reads were quality-assessed with NanoPlot (De Coster et al., 2018); De novo genome assemblies were generated using Flye(Kolmogorov et al., 2019), and genome annotation was performed with Bakta (Schwengers et al., 2021). Assembly completeness and contamination were evaluated using CheckM v1.2.2(Parks et al., 2015). Using lineage-specific marker genes, whole-genome taxonomic assignment was performed with the Type Strain Genome Server (TYGS). Whole-genome taxonomic assignment was conducted using the Type (Strain) Genome Server (TYGS) platform (Meier-Kolthoff & Göker, 2019).

Establishment of Organic acid and phosphorus treatments

Throughout this study, soluble phosphorus (P+) refers to readily available orthophosphate, whereas poorly soluble phosphorus (P−) refers to P associated with sparingly soluble mineral phases that require acidification, Ca^{2+} chelation, and/or enzymatic activity for mobilization (Kalayu, 2019). A modified version of the minimal culture medium (MCM) described by Barra et al. (2019) was prepared with the following composition (per liter): NH_4Cl (4.3 g), KCl (1 g), $CaCl_2{\cdot}2H_2O$ (10 mg), K_2SO_4 (0.87 g), H_3BO_3 (1 mg), $MnSO_4$ (1.114 mg), $ZnSO_4{\cdot}7H_2O$ (12.6 mg), $CuSO_4{\cdot}5H_2O$ (7.822 mg), MoO_3 (1 mg), $FeSO_4{\cdot}7H_2O$ (1.6 µg), and $MgSO_4{\cdot}7H_2O$ (0.49 g). P was supplied at a final concentration of 1.4 mM, either as KH_2PO_4 (pKa 6.86) representing soluble P (P+), or as $Ca_3(PO_4)_2$ (Ksp = 2.1×10^{-33} at 25°C), representing poorly soluble P (P-). Citric, malic, and oxalic acids were added individually as the experimental LMWOA treatments. Emphasis was placed on bacterial responses under poorly soluble phosphorus (P−), as this condition more closely represents the P limitations characteristic of Andisol soils. All media were buffered to pH 5.4 using 0.0667 M potassium phthalate ($C_8H_5KO_4$). Organic acid concentrations were selected based on concentrations previously reported for *Lolium perenne* root exudates to ensure ecological relevance (Mingji et al., 2009; Mora et al., 2009; Parra-Almuna et al., 2024).

Evaluation of Bacterial Growth

An overnight culture of phosphobacteria was grown in liquid LB medium. Cells were subsequently harvested by centrifugation, and the resulting pellet was washed with sterile distilled water to remove residual LB medium. The washed cells were then inoculated into a fresh minimal culture medium supplemented

with the corresponding organic acid and incubated overnight for acclimation. This preconditioning period was included to minimize the physiological stress associated with the abrupt transition from the nutrient-rich LB medium to the nutrient-limited experimental medium, thereby reducing its potential influence on the subsequent growth kinetics. Following acclimation, the OD_{600} of each culture was measured and used to calculate the inoculum volume required to obtain an initial OD_{600} of 0.2–0.4 in the subsequent growth assay. The calculated volume of each culture was harvested by centrifugation, washed with sterile distilled water to minimize carryover of compounds from the acclimation medium, and resuspended in fresh minimal medium containing the corresponding organic acid treatment. The resulting bacterial suspensions were inoculated into 96-well plates following the methodology described by Mira et al., (2022). Bacterial growth was monitored by measuring OD_{600} every 6 h for 48 h under standard incubation conditions. Growth kinetics and growth rates were subsequently determined from the OD_{600} measurements using the R packages growthrates and gcplyr (Blazanin, 2023).

Gene Expression Analysis under Organic-Acid Treatments

Based on growth-curve assays, bacterial isolates exhibiting the highest growth under conditions of poorly soluble P (P-) were selected for gene expression analysis. After exposure to the selected organic-acid treatments, total RNA was extracted from the phosphobacteria isolate using Trizol reagent following the manufacturer's instructions, with minor modifications to preserve RNA integrity: all reagents were pre-chilled before use, and samples were handled on ice throughout the extraction process. First-strand cDNA was synthesized from total RNA using M-MLV reverse transcriptase (Promega) according to the supplier's protocol. Quantitative real-time PCR (qRT-PCR) was conducted using SYBR Green chemistry (Thermo Fisher Scientific) on a QuantStudio 3 system. Genes associated with P acquisition and metabolism were identified through genome annotation. Based on their predicted functions and genomic distribution among the evaluated isolates, *phoA, phoE*, and *pstS* were selected for expression analyses in all strains. Gene expression analyses were restricted to poorly soluble P (P^-) treatments that supported bacterial growth. The 16S rRNA gene was used as the reference gene for normalization and was amplified using the universal primer pair Bac1369F (5'-CGG TGA ATA CGT TCY CGG-3') and Prok1492R (5'-GGW TAC CTT GTT ACG ACT T-3') (Suzuki et al., 2000). Relative transcript abundance was calculated using the $2^{-\Delta\Delta Ct}$ method (Pfaffl, 2001), with the corresponding soluble P (P^+) treatment used as a control corresponding to each treatment.

Table 1
List of primers sequences used for quantitative real-time polymerase chain reaction (qRT-PCR) analysis of phoA, phoE and pstS genes.

Specie	Gene name	Forward primer (5' -> -3')	Reverse primer (5' -> -3')
Klebsiella michiganensis	*phoA*	GGCGCTGAACACCAAAGATG	GTGCGGCTTTCATGGTGTAG
	phoE	TTTATGACCAAACGCGCCAG	CGTCGCCGTTCTGTTTCTTG
	pstS	GCATGGCCGATCACTTCAAC	CTTGCTCAACCACGCTTTCC
Enterobacter ludwigii	*phoA*	TGTCACCTCGCGTAAATGCT	CGGTTTCCGCGAAGGTTTTC
	phoE	AAAGCAGAAGCATGGGCAAC	GACGCAGACCGAAATCGAAC
	pstS	GTTCGTCGTGCAGATGGTTC	GTCGTTGCCTTTACCACCCA
Genes obtained by complete genome by Nanopore sequencing			

Quantification of dissolved P in culture medium

The concentration of soluble inorganic P (Pi) in bacterial culture supernatants was determined using an adaptation of the molybdenum blue colorimetric method described by Murphy and Riley (1962). Briefly, reagent and sample volumes were proportionally reduced to allow analysis in a 96-well microplate format, using 200 µL of sample and 40 µL of colorimetric reagent per well. Before sampling, the culture medium was thoroughly homogenized, and a 1 mL aliquot was collected from each treatment. Samples were centrifuged at 12,000 × g for 3 min, and only the supernatant was used for soluble P determination. Prior to absorbance measurement, the microplate was briefly shaken in the microplate reader to ensure homogeneous mixing and eliminate air bubbles that could interfere with the readings. Absorbance was measured at 880 nm at the initial sampling time (Ti) and at the gene expression sampling time (Tf) for each treatment.

Comparative genomic analysis

Comparative genomic analyses were performed to identify genes associated with P acquisition and metabolism, plant growth-promoting traits, and organic acid utilization. Genomes were initially annotated using Bakta. Functional assignments were subsequently refined using EggNOG-mapper, and predicted proteins were screened based on Kyoto Encyclopedia of Genes and Genomes (KEGG) Orthology (KO) annotations obtained through the KEGG database and associated tools (Kanehisa, 2002). Gene inventories were compared among isolates to identify conserved and strain-specific functions. Attention was given to genes involved in P and organic acid metabolism. These analyses were used to complement physiological and transcriptional observations and to identify candidate genes potentially involved in the differential responses observed under organic acid treatments.

Statistical analysis

All statistical analyses and graphical representations were performed in R (version 4.5.1).

Growth curves were visualized using the ggplot2 package. Mean optical density (OD_{600}) values and standard deviations were calculated from biological replicates and used for graphical representation. Growth data were used to identify representative organic-acid concentrations for subsequent gene expression analyses and were not subjected to inferential statistical testing.

Relative gene expression ($2^{-\Delta\Delta Ct}$) values were analyzed independently for each bacterial isolate and target gene. Prior to statistical analyses, amplification failures (undetermined reactions) were excluded. Normality and homogeneity of variances were assessed using the Shapiro–Wilk and Levene tests, respectively. Gene expression data were analyzed using two-way analysis of variance (ANOVA), with organic acid, concentration, and their interaction as fixed factors. Significant differences among treatment combinations were determined using estimated marginal means (emmeans) followed by Tukey-adjusted pairwise comparisons. Differences were considered statistically significant at $p < 0.05$.

Principal component analysis (PCA) was performed separately for each bacterial isolate using mean fold change ($2^{-\Delta\Delta Ct}$) values to evaluate overall patterns of gene expression across organic acid treatments and concentrations.

Soluble P data were analyzed independently for each organic acid. Differences between the control and bacterial treatments, as well as among organic acid concentrations within each bacterial strain and sampling time, were evaluated using one-way ANOVA followed by Tukey's HSD post hoc test ($p < 0.05$). Differences between the initial (T_i) and final (T_f) sampling times for each bacterial strain, organic acid, and concentration were assessed using Student's t-test.

Results

Phosphobacteria complete genome sequencing

Phylogenomic analysis of whole-genome sequences generated with Oxford Nanopore technology and analyzed on the TYGS platform assigned strains RC3 and RCJ4 to *Klebsiella michiganensis*, whereas RJAL6_2 was assigned to *Enterobacter ludwigii* (Supplementary figure S1). These assignments were supported by genome-wide comparisons with type strains and phylogenomic reconstruction using Genome BLAST Distance Phylogeny (GBDP), yielding higher taxonomic resolution than previous classifications based on partial 16S rRNA gene sequences or draft genome assemblies (Supplementary table S1).

The three genomes exhibited high completeness and without contamination, enabling reliable species-level identification. The genome assembly metrics are summarized in Table 2. The RC3 genome was assembled into three circular replicons corresponding to a complete chromosome, one megaplasmid, and one plasmid, with CheckM estimating 95.92% completeness for the complete assembly, including all three replicons. RCJ4 and RJAL6_2 were assembled into near-complete genomes, with 100% completeness. The improved assembly quality obtained using long-read sequencing facilitated more accurate taxonomic assignment.

Table 2
Summary of genome assembly characteristics and sequencing coverage for the bacterial strains analyzed

Strain	Technology of sequencing	Genome size	Number of contigs	GC%	Coverage	Completeness
RC3	Nanopore MinION R10.4.1	6.09 Mb	3	56	~ 13x	95.92%
RCJ4		6.3 Mb	6	56	~ 86x	100%
RJAL6_2		5.01 Mb	5	54	~ 104x	100%

Bacterial growth under organic acid treatments

Bacterial growth dynamics varied according to organic acid concentration under poorly soluble P conditions (Fig. 1). Growth rates were estimated using the slope obtained from the linear regression of log10-transformed OD_{600} values over time. Differences in slope values among treatments reflected variations in bacterial growth associated with organic acid concentration and P availability (Supplementary table and figure S2). In general, lower slopes were observed at the lowest concentration tested (0.1 mM), suggesting that organic acid availability may represent a limiting factor for bacterial metabolism under these conditions. Intermediate concentrations (1 mM) frequently yielded higher slopes, indicating that this concentration range supported more favorable growth conditions for most isolates. At the highest concentration tested (20 mM), several treatments showed reduced slopes, which may reflect metabolic saturation or physiological stress associated with elevated organic acid concentrations.

No detectable bacterial growth was observed in the organic acid-free controls, regardless of whether soluble (P+) or poorly soluble P (P−) was supplied. During the acclimation step, none of the three isolates exhibited visible turbidity in media containing only the buffer and the corresponding P source, in contrast to cultures supplemented with citric, malic, or oxalic acid. Consequently, the organic acid-free cultures did not reach sufficient cell densities to be standardized to the initial OD_{600} required for the growth assay and could not be included in the subsequent growth kinetics. Based on the growth assay results, three organic acid concentrations (0.1, 1, and 20 mM), representing low, intermediate, and high concentrations, were selected for subsequent gene expression analyses.

Expression of phosphate-related genes under P^- conditions

In *K. michiganensis* RC3, two-way ANOVA revealed significant effects of organic acid identity ($p = 0.0088$), concentration ($p < 0.0001$), and their interaction ($p < 0.0001$) on *phoA* expression (Supplementary Table S3; Fig. 2). The highest expression was observed under 20 mM citric acid, reaching approximately a 6-fold increase relative to the control and differing significantly from all remaining treatments. In contrast, expression was significantly reduced under 1 mM citric and 1 mM oxalic acid, whereas no amplification was detected in the presence of 0.1 or 20 mM malic acid. For *phoE*, significant effects were also

detected for organic acid identity, concentration, and their interaction (all $p < 0.0001$). The greatest induction occurred with 0.1 mM oxalic acid (approximately 6-fold above the control), whereas the strongest repression was observed under 20 mM citric acid (approximately 20-fold lower than the maximum expression). Intermediate expression levels were detected under 1 mM and 0.1 mM citric acid. In contrast, *pstS* expression was significantly affected by concentration ($p < 0.0001$) and by the interaction between organic acid and concentration ($p < 0.0001$), whereas the main effect of organic acid alone was not significant ($p = 0.328$). The highest expression was observed under 0.1 mM malic and 0.1 mM oxalic acid, both showing approximately a 2-fold increase relative to the control and not differing significantly from each other. Expression progressively declined at higher organic acid concentrations, reaching its lowest level under 20 mM citric acid.

In *K. michiganensis* RCJ4, two-way ANOVA revealed significant effects of organic acid identity, concentration, and their interaction on *phoA* expression (all $p < 0.0001$; Supplementary Table S3; Fig. 2). The strongest induction occurred under 1 mM malic acid (approximately 7-fold relative to the control), although expression under 0.1 mM citric acid did not differ significantly from this treatment. The lowest expression was observed under 20 mM malic acid, whereas no amplification was detected under 0.1 mM oxalic acid. Similarly, *phoE* expression was significantly affected by organic acid identity, concentration, and their interaction (all $p < 0.0001$). Expression reached its highest level under 20 mM oxalic acid (approximately 8-fold relative to the control), followed by 0.1 mM citric acid. The greatest reduction occurred under 1 mM citric acid, while no amplification was detected under 0.1 mM malic and oxalic acid. Likewise, *pstS* expression was significantly influenced by organic acid identity ($p < 0.0001$), concentration ($p = 0.0003$), and their interaction ($p < 0.0001$). The highest expression was observed under 0.1 and 1 mM malic acid and 20 mM oxalic acid, which did not differ significantly from one another. Conversely, the lowest expression was observed under 0.1 mM citric acid.

In *E. ludwigii* RJAL6_2, two-way ANOVA revealed significant effects of organic acid identity ($p < 0.0001$), concentration ($p < 0.0001$), and their interaction ($p < 0.0001$) on *phoA* expression (Supplementary Table S3; Fig. 2). The highest relative expression was observed under 1 mM citric acid (approximately 16-fold relative to the control), although expression under 20 mM oxalic acid (approximately 10-fold) did not differ significantly from this treatment. The lowest relative expression occurred under 1 and 20 mM malic acid, whereas no amplification was detected under 0.1 mM malic acid. For *phoE*, significant effects were also detected for organic acid identity ($p < 0.0001$), concentration ($p = 0.0001$), and their interaction ($p < 0.0001$). Expression was highest under 20 mM oxalic acid and 1 mM citric acid, which did not differ significantly from each other and both exhibited approximately 16-fold higher expression than the control. All remaining treatments showed significantly lower expression. Similarly, *pstS* expression was significantly affected by organic acid identity ($p < 0.0001$), concentration ($p = 0.0006$), and their interaction ($p < 0.0001$). The highest expression was observed under 1 mM citric acid (approximately 8-fold relative to the control) and 20 mM oxalic acid (approximately 5-fold), which did not differ significantly from one another, whereas the lowest expression was observed under 1 mM malic acid.

Comparison of the three bacterial strains revealed distinct transcriptional responses to the evaluated LMWOAs (Fig. 3). Principal component analysis explained 93.0% (PC1 = 67.0%, PC2 = 26.0%), 74.6% (PC1 = 45.1%, PC2 = 29.5%), and 97.9% (PC1 = 90.7%, PC2 = 7.2%) of the total variation in gene expression for *K. michiganensis* RC3, *K. michiganensis* RCJ4, and *E. ludwigii* RJAL6_2, respectively. Across treatments, RJAL6_2 exhibited the strongest induction of P acquisition genes, reaching the highest fold changes for *phoA*, *phoE*, and *pstS*. In contrast, both *Klebsiella* isolates displayed more heterogeneous expression profiles, with the maximum expression of each gene occurring under different organic acid treatments. The hierarchical clustering analysis (Supplementary Fig. S3) further supported these transcriptional differences by showing coordinated expression of *phoA*, *phoE*, and *pstS* in RJAL6_2, whereas both *Klebsiella* isolates exhibited more heterogeneous gene-expression profiles.

Quantification of dissolved P in culture medium

When comparing soluble P concentrations among treatments (Control, RC3, RCJ4, and RJAL6_2; lowercase letters), significant differences depended on the organic acid, concentration, and sampling time (Fig. 4). Under citric acid, significant differences among treatments were detected at 0.1 and 1 mM during Ti ($p < 0.0001$ and $p = 0.0013$, respectively), with additional differences detected at 20 mM ($p < 0.0001$). At Tf, significant differences were detected only at 1 mM ($p = 0.0146$), whereas no significant differences were observed at 0.1 or 20 mM. Under malic acid, significant differences among treatments were detected at all concentrations during Ti ($p = 0.0017–0.0307$), whereas at Tf significant differences were detected only at 0.1 and 20 mM ($p = 0.0115$ and $p = 0.0083$, respectively). Similarly, under oxalic acid, significant differences among treatments were detected at all concentrations during Ti ($p = 0.0070–0.0110$), whereas at Tf significant differences were detected only at 0.1 mM ($p = 0.0002$).

Comparison among concentrations within each strain (capital letters) revealed a significant effect of concentration for all treatments, organic acids, and sampling times (one-way ANOVA, all $p \leq 0.0007$). For citric and oxalic acids, the highest soluble P concentrations were generally observed at 0.1 and 1 mM, whereas malic acid most frequently reached its highest soluble P concentration at 1 mM. In contrast, the highest organic acid concentration (20 mM) generally resulted in the lowest soluble P concentrations across treatments. Comparison between sampling times (Ti and Tf; asterisks) identified significant differences for a limited number of treatment combinations, including RC3 supplemented with 1 mM citric acid ($p = 0.0009$), RC3 supplemented with 0.1 and 1 mM oxalic acid ($p = 0.0207$ and $p = 0.0308$, respectively), RCJ4 supplemented with 20 mM oxalic acid ($p = 0.0014$), and RJAL6_2 supplemented with 0.1 and 20 mM citric acid ($p = 0.0080$ and $p = 0.0008$, respectively), 20 mM malic acid ($p = 0.0096$), and 1 mM oxalic acid ($p = 0.0057$).

Pairwise comparisons among organic acids (Supplementary Table S4; uppercase letters with primes) detected significant differences only for selected treatment combinations. Specifically, significant differences among citric, malic, and oxalic acids were detected in RC3 at 1 mM (Ti, $p = 0.0016$; Tf, $p = 0.0129$) and 20 mM (both sampling times, $p < 0.0001$), in RCJ4 at 20 mM (both sampling times, $p < 0.0001$), and in RJAL6_2 at 1 mM (Ti, $p = 0.0029$; Tf, $p = 0.0042$) and 20 mM (both sampling times, $p < 0.0001$). No significant differences among organic acids were detected for the remaining treatment combinations.

Comparative genomic analysis of phosphorus- and organic acid-related genes in phosphate-solubilizing bacteria

Comparative genomic analysis revealed that all three P-solubilizing bacteria harbor a conserved set of genes involved in P acquisition and regulation, including the Pho regulon components (*phoB*, *phoR*, *phoU*, *phoE*, and *phoA*) and the high-affinity phosphate transport system (*pstSABC*). In addition, all strains possessed the core phosphonate utilization genes (*phnCDEJP*), suggesting the ability to access alternative P sources under P-limiting conditions. However, notable differences were observed among the isolates. The genes *gcd*, *appA*, and *pitA* were detected exclusively in RC3 and RCJ4, whereas they were absent in RJAL6_2. The presence of *gcd* indicates the potential to solubilize mineral phosphate via glucose oxidation, while *appA* encodes an acid phosphatase/phytase that hydrolyzes organic P compounds. Likewise, *pitA* provides an additional low-affinity phosphate uptake system. Collectively, the genomic comparisons indicate that RC3 and RCJ4 possess a broader repertoire of P-acquisition mechanisms than RJAL6_2, potentially conferring greater metabolic flexibility under variable P availability. In addition, comparative genome annotation revealed a high degree of conservation across both P- and organic acid-related metabolic pathways, although several genes involved in P acquisition were strain-specific. A comprehensive overview of the distribution of genes associated with P and organic acid metabolism, together with the number of annotated genes within each functional category, is presented in Fig. 5.

As shown in Fig. 5, the three isolates exhibited a highly conserved genomic repertoire associated with the sensing, transport, and metabolism of LMWOAs. Genes involved in citrate sensing and utilization (*citA* and *citB*), dicarboxylate transport (*dctA*), tricarboxylate transport (*tctA*, *tctC*, and *tctE*), and malate uptake (*maeN*) were present in all strains. Likewise, all genomes encoded key enzymes of the tricarboxylic acid cycle and related metabolic pathways, including *acnA*, *acnB*, *fumC*, *mdh*, *mqo*, *maeA*, and *maeB*, which participate in the interconversion of citrate, malate, fumarate, oxaloacetate, and pyruvate. The conservation of these genes indicates that RC3, RCJ4, and RJAL6_2 share a substantial genetic potential to detect, transport, and metabolize plant-derived organic acids, such as citrate and malate. Therefore, any physiological differences observed among the strains in response to organic acid supplementation are more likely attributable to differences in gene regulation, expression patterns, or metabolic efficiency rather than to the absence of major transport or catabolic pathways.

Discussion

The present study shows that LMWOAs exert distinct effects on bacterial growth and P-acquisition gene expression in P-solubilizing bacteria. While citric and malic acids primarily promoted bacterial growth in the two *Klebsiella* isolates, oxalic acid induced a coordinated increase in the expression of *phoA*, *phoE*, and *pstS* in *E. ludwigii* RJAL6_2 despite its comparatively lower growth. Comparative genomic analyses further revealed that the three isolates share a highly conserved repertoire of genes involved in P acquisition and LMWOAs metabolism. Consistent with the absence of bacterial growth in medium containing phthalate buffer without LMWOAs, no genes associated with known phthalate degradation pathways were identified in the annotated genomes. Together, these findings suggest that the physiological differences observed among strains may be associated primarily with differences in regulatory responses rather than with their genomic potential.

Previous studies have demonstrated that both the composition and quantity of LMWOAs exuded by *Lolium perenne* vary according to soil chemical properties and environmental stress. Under manganese toxicity in acidic Andisols, oxalic acid consistently represents the dominant root exudate, followed by citric and malic acids, with exudation increasing as Mn availability increases Mora et al. (2009). Similarly, Mingji et al. (2009) reported enhanced oxalate exudation by *L. perenne* growing in phenanthrene-contaminated soils, whereas Rosas et al. (2011) demonstrated that P deficiency significantly increases the exudation of oxalic, citric, and malic acids, with oxalate remaining the predominant compound under all treatments. Consistent with these observations, oxalic acid was also the predominant LMWOAs detected in the present study, whereas malic and citric acids were exuded at substantially lower rates. The highest exudation levels were generally observed under manure fertilization, reinforcing previous evidence that root exudation patterns are strongly influenced by nutrient availability and soil management (Wang, Gao, et al., 2023; Yang et al., 2026). Differences in root exudate composition were accompanied by marked physiological differences among the P-solubilizing bacteria evaluated. Although both *Klebsiella* isolates displayed enhanced growth in the presence of citric and malic acids, *E. ludwigii* RJAL6_2 exhibited approximately two-fold lower growth when oxalic acid was supplied as the sole carbon source. These observations indicate that individual LMWOAs do not represent equivalent carbon substrates for different rhizosphere bacteria and are consistent with species-specific metabolic capabilities governing carbon utilization.

This interpretation is supported by recent evidence demonstrating that soil microorganisms preferentially consume LMWOAs over sugars as readily available carbon sources (Wiesenbauer et al., 2025). Importantly, these authors also demonstrated that different organic acids stimulate distinct microbial metabolic responses, indicating that microbial activity depends not only on carbon availability but also on the chemical identity of the exuded compounds. Likewise, Menezes-Blackburn et al. (2016) proposed that root-derived LMWOAs simultaneously regulate P availability and microbial community composition, whereas Al-Kalbani et al. (2025) showed that environmental stresses such as salinity alter microbial utilization of LMWOAs and consequently reshape soil microbial communities. Together, these findings support the hypothesis that individual LMWOAs represent chemically distinct ecological signals rather than interchangeable carbon substrates.

Because relatively few studies have directly examined the effects of individual LMWOAs on the P-acquisition in soil microorganisms (Wei et al., 2018; Zhang et al., 2021; Zheng et al., 2026; Zhi et al., 2025), additional ecological context can be drawn from studies investigating microbial carbon utilization in natural soil ecosystems. Recent work in Andisols from native forests and Pinus radiata plantations under pre- and post-wildfire conditions demonstrated that soil microbial communities differentially utilized malic, citric, and oxalic acids depending on soil conditions (De Ferrari et al., 2026; Merino-Guzmán et al., 2026). Although these studies were conducted in ecosystems distinct from the *Lolium perenne* rhizosphere and did not evaluate P-acquisition gene expression, they reinforce the concept that soil microorganisms do not utilize all LMWOAs equivalently. Rather, substrate utilization appears to depend on environmental conditions and the metabolic requirements of the microbial community. This broader ecological perspective is consistent with our observations that the

three phosphate-solubilizing isolates exhibited distinct physiological responses to citric, malic, and oxalic acids despite sharing a highly conserved repertoire of genes involved in P-acquisition and LMWOAs metabolism.

The physiological differences observed among isolates cannot be explained solely by differences in their annotated genomic potential. Comparative genome analysis revealed that all three bacteria harbor a highly conserved repertoire of genes involved in P sensing and acquisition, including the complete Pho regulon (*phoB, phoR, phoU, phoE*, and *phoA*), the high-affinity phosphate transport system (*pstSABC*), and phosphonate utilization genes (*phnCDEJP*). Likewise, all genomes encoded the major transport systems and metabolic pathways required for the uptake and utilization of citrate and malate, including *citAB, dctA, tctACE*, and *maeN*, together with the core enzymes of the tricarboxylic acid cycle. In contrast, no canonical genes associated with oxalate catabolism were identified, despite all three isolates exhibiting measurable growth in an oxalate-containing medium. This apparent discrepancy raises the possibility that oxalate utilization may involve alternative transport systems, enzymes with broader substrate specificity, or metabolic pathways that remain poorly characterized in Enterobacterales.

Although RC3 and RCJ4 uniquely possessed *gcd, appA*, and *pitA*, the overall conservation of P-related pathways, together with the genes involved in citrate and malate transport and metabolism, indicates that all three isolates share a broadly similar genetic potential for P acquisition and LMWOAs utilization. Therefore, the contrasting physiological responses observed in this study are more likely attributable to differences in gene regulation, metabolic efficiency, or signal perception, rather than the absence of major metabolic pathways. One of the most notable findings of this study was that bacterial growth did not directly predict transcriptional activation of P-acquisition genes. Under oxalic acid supplementation, *E. ludwigii* RJAL6_2 exhibited one of the lowest growth rates while simultaneously showing coordinated overexpression of *phoA, phoE*, and *pstS*. This observation suggests that bacterial proliferation and P-acquisition responses may become partially uncoupled under specific environmental conditions.

One possible explanation is that under oxalate exposure, a larger proportion of cellular resources is allocated toward P mobilization and transport rather than biomass production. Interestingly, similar metabolic characteristics have been reported for *Enterobacter bugandensis* UFPI B5-6, which preferentially produces citric and malic acids over oxalic acid during P solubilization (de Almeida Leite et al., 2024). Consequently, oxalate may represent a specific environmental signal capable of inducing regulatory responses in *Enterobacter*, rather than functioning solely as a preferred carbon source. Collectively, these findings support the hypothesis that changes in root exudate composition contribute not only to the shaping of rhizosphere microbial communities but also to the regulation of their functional activity. Within this framework, citric and malic acids appear to preferentially stimulate bacterial proliferation, whereas oxalic acid promotes the transcriptional activation of genes involved in P acquisition by the bacteria. Such differential responses may allow plants to regulate not only the abundance of beneficial microorganisms but also their metabolic functions, thereby maintaining microbial populations in a physiologically active state without necessarily maximizing bacterial growth.

This interpretation is consistent with the growing recognition that root exudates function as signaling molecules that coordinate plant–microbe interactions. Wei et al. (2018) demonstrated that LMWOAs modify microbial community composition and indirectly regulate P availability by altering bacterial interactions. More recently, (Wang, Luo, et al., 2023) reported that root-derived LMWOAs regulate the abundance and diversity of *phoD*-harboring bacteria, particularly *Pseudomonas* and *Bacillus*, thereby increasing alkaline phosphatase activity and enhancing P mobilization. Together with our results, these studies support the view that LMWOAs integrate chemical mobilization of P with biological regulation of P-acquisition pathways.

Another important finding was that transcriptional responses were highly strain-specific. Previous genomic analyses identified a high degree of conservation of the *phoU–pstSCAB* phosphate transport system and other P-acquisition pathways in *K. michiganensis* and *E. ludwigii* isolates recovered from Chilean Andisols (Cortés-Albayay et al., 2024). Nevertheless, the three isolates evaluated here exhibited markedly different growth patterns and gene-expression profiles under identical experimental conditions. A comparable trend was observed in the proteomic analyses of (Barra et al., 2023), where proteins associated with the core P-acquisition machinery, including *phoA, phoE*, and *pstS*, were consistently induced under P-deficient conditions, whereas broader metabolic responses varied among bacterial isolates. Although these studies were conducted under different experimental conditions, they collectively illustrate that isolates belonging to the same bacterial species may exhibit distinct physiological, proteomic, and transcriptional responses despite sharing a highly conserved P-acquisition machinery. Even the two *K. michiganensis* isolates evaluated here responded differently to the same LMWOAs despite possessing nearly identical P-acquisition pathways. Principal component analysis further supported these strain-specific transcriptional responses by revealing distinct global expression patterns for each bacterial isolate. In RC3, the PCA showed an inverse relationship between *phoA* and the combined expression pattern of *phoE* and *pstS*, indicating that treatments associated with increased *phoA* expression tended to exhibit lower expression of the other two genes, and vice versa. A similar inverse relationship was observed in RCJ4; however, the associated treatments differed, resulting in a distinct spatial distribution of the gene vectors. In contrast, *E. ludwigii* RJAL6_2 exhibited a strong positive association between *phoA* and *phoE*, whereas *pstS* was oriented in the opposite direction, indicating that treatments promoting *phoA* and *phoE* expression were generally associated with reduced *pstS* expression.

Although soluble P concentrations varied among bacterial treatments and organic acids, these changes did not consistently reflect the transcriptional patterns observed for P-acquisition genes. In several cases, treatments with comparable soluble P concentrations exhibited contrasting expression profiles, indicating that soluble P availability alone cannot fully explain the observed transcriptional responses. Interestingly, increasing the concentration of LMWOAs did not consistently increase soluble P. By contrast, the highest organic acid concentrations frequently resulted in lower soluble P values than intermediate concentrations, suggesting that the relationship between LMWOAs concentration and P solubilization is not linear. One possible explanation involves the pH-dependent speciation of organic acids rather than treatment-induced changes in medium pH. The culture medium remained effectively buffered at approximately pH 5.4 throughout the experiment, with no substantial changes between the initial and final sampling times. Under these conditions, malate and citrate are not completely deprotonated, whereas oxalate occurs predominantly in its divalent form. Differences in P availability among treatments are therefore unlikely to result from differential acidification of the medium and may instead reflect differences in LMWOAs concentration, speciation, and Ca^{2+}-complexing capacity. Because ligand complexation is strongly influenced by the protonation state of organic acids, their interactions with Ca^{2+} and,

consequently, their capacity to promote dissolution of calcium phosphate may differ under the experimental conditions used here (Luo et al., 2025; Moropana et al., 2026).

Several studies (Dabare et al., 2026; Luo et al., 2025; Moropana et al., 2026) have shown that excessive concentrations of organic acids may reduce the amount of soluble P through secondary precipitation processes. Rapid dissolution of calcium phosphate can locally generate high concentrations of both Ca^{2+} and phosphate ions. When these ions exceed their solubility threshold, secondary calcium phosphate phases may precipitate, thereby reducing the concentration of P remaining in solution, despite continued mineral dissolution. Similarly, excessive oxalate or citrate concentrations may alter calcium complexation dynamics. High oxalate concentrations can promote the formation of calcium oxalate surfaces capable of adsorbing phosphate, whereas excessive citrate may reduce the stability of soluble calcium-citrate complexes by competing for solvation water, ultimately favoring P precipitation (Dabare et al., 2026; Moropana et al., 2026). Although these mechanisms were not directly evaluated in the present study, they provide plausible explanations for the lower soluble P concentrations observed at the highest LMWOAs concentrations.

From an ecological perspective, precipitation processes may have important implications for rhizosphere P dynamics. Rather than maximizing the instantaneous concentration of soluble P, high concentrations of LMWOAs may promote a slower and more sustained P release by maintaining a larger pool of sparingly soluble P that remains available for gradual dissolution over time. In plant–soil systems, this could prolong P availability while simultaneously modulating bacterial gene expression through changes in root exudation patterns. Consequently, optimizing organic acid exudation may require balancing immediate P mobilization with long-term P availability, depending on the agronomic objective. Together, these observations indicate that genomic potential alone is insufficient to predict bacterial behavior under P limitation. Although all three isolates possess highly similar P-acquisition pathways, differences in soluble P dynamics and global transcriptional patterns highlight the importance of regulatory architecture, transcriptional control, and metabolic efficiency play fundamental roles in determining how individual phosphobacteria respond to rhizosphere-derived chemical signals. This interpretation agrees with (Bergkemper et al., 2016), who demonstrated that P-acquisition strategies vary substantially even among closely related bacterial taxa.

Interestingly, the highest organic acid concentration evaluated in this study (20 mM) falls within the range reported to inhibit the growth of several bacterial pathogens, including *Escherichia coli, Salmonella enterica, Staphylococcus aureus*, and *Listeria monocytogenes* (Ji et al., 2023; Karpiński & Ożarowski, 2024). Nevertheless, all three P-solubilizing isolates remained capable of growth under at least some of the 20 mM treatments, while simultaneously maintaining elevated expression of P-acquisition genes. These findings indicate that the biological effects of LMWOAs strongly depend on bacterial identity and ecological context. Rather than acting exclusively as antimicrobial compounds, root-derived organic acids may serve as selective carbon substrates and signaling molecules for microorganisms adapted to the rhizosphere environment.

Although this study provides novel insights into the effects of individual LMWOAs on P-solubilizing bacteria, the experimental design represents a simplified model of rhizosphere conditions. Organic acids were supplied individually under controlled laboratory conditions, whereas natural root exudates comprise complex mixtures of metabolites that fluctuate dynamically throughout plant development. Likewise, plant–soil–microorganism interactions involve numerous biological, chemical, and physical processes that cannot be fully reproduced under *in vitro* conditions. Nevertheless, isolating these variables provides a valuable mechanistic framework for identifying the individual factors that influence bacterial growth, P solubilization, and P-acquisition gene expression in response to individual LMWOAs.

Future research should build upon this reductionist approach by incorporating P-deficient Andisols, plants, and P-solubilizing bacteria into controlled greenhouse experiments. Such studies would enable the evaluation of how root exudation patterns under different fertilization regimes influence bacterial colonization, P solubilization, gene expression, and plant P acquisition within a more realistic rhizosphere environment. Integrating these biological and physicochemical measurements would help validate the regulatory role of LMWOAs under conditions that more closely resemble natural plant–soil–microorganism interactions.

Taken together, our findings demonstrate that LMWOAs should not be regarded solely as carbon sources or chemical agents involved in P-solubilization. Instead, they appear to function as environmentally derived signaling molecules that differentially regulate bacterial growth and P-acquisition pathways according to the bacterial identity and regulatory capacity. By integrating root exudation patterns, comparative genomics, bacterial physiology, and gene expression analyses, this study provides a mechanistic framework for understanding how plants regulate the functional behavior of P-solubilizing bacteria through modifications in root exudate chemistry under P-limited conditions.

Conclusions

This study characterized the physiological, transcriptional, and genomic responses of three native phosphate-solubilizing bacteria isolated from Chilean volcanic Andisols (*K. michiganensis* RC3 and RCJ4, and *E. ludwigii* RJAL6_2) following exposure to the three predominant LMWOAs reported in Lolium perenne root exudates under P-deficient conditions. The results showed that citric, malic, and oxalic acids differentially influenced bacterial growth and the expression of P-acquisition genes, revealing marked strain-dependent responses.

Comparative genomic analyses revealed that the three isolates shared a highly conserved repertoire of genes involved in P acquisition, transport, and LMWOAs metabolism, suggesting that the contrasting physiological and transcriptional responses observed among isolates are more likely associated with differences in regulatory mechanisms than with the presence or absence of major metabolic pathways. One of the most notable findings was that bacterial growth and P-acquisition gene expression were not necessarily coupled. Whereas citric and malic acids generally promoted bacterial growth, oxalic acid was associated with coordinated expression of *phoA, phoE*, and *pstS* in *E. ludwigii* RJAL6_2 despite comparatively reduced growth. Collectively, these observations support the hypothesis that individual LMWOAs may differentially modulate P-acquisition responses in a strain-dependent manner.

The observation that increasing LMWOAs concentration did not consistently increase soluble P further highlights the importance of considering P-release dynamics, rather than instantaneous soluble P concentrations, when evaluating the ecological role of root exudates. Likewise, the transcriptional responses observed in this study could not be explained solely by differences in soluble P availability. Treatments exhibiting comparable soluble P concentrations frequently displayed contrasting expression profiles, whereas changes in gene expression were more consistently associated with the identity of the LMWOAs supplied. Together, these findings suggest that, under P-deficient conditions, individual LMWOAs may contribute to the modulation of bacterial P-acquisition responses beyond their established roles as carbon sources and P-solubilizing agents.

By integrating bacterial physiology, comparative genomics, transcriptional responses, soluble P dynamics, and bacterial growth, this study provides a mechanistic framework for understanding how variation in root exudate chemistry may influence the functional behavior of phosphate-solubilizing bacteria under P-deficient conditions. The present findings suggest that the identity of individual LMWOAs may represent an additional factor influencing bacterial P-acquisition strategies beyond P limitation alone. These results provide a foundation for future greenhouse and field studies aimed at evaluating how root exudate chemistry influences P cycling and plant–microorganism interactions in agricultural soils. A better understanding of these bacterial responses may also contribute to the development of agronomic strategies that improve P-use efficiency, optimize nutrient management, and promote the conservation and effective use of native beneficial microbial reservoirs to enhance crop productivity in P-limited soils.

Declarations

AI Use Statement

NotebookLM (Google) was used to assist in the creation and refinement of the graphical abstract, while ChatGPT (OpenAI, GPT-5.5) was used to assist with prompt development and R script refinement. All scientific content, data analysis, interpretation, and final approval were performed by the authors.

Additional Information (including a Competing Interests Statement)

MLM is an inventor on International Patent Application No. WO/2026/060538, which includes the RC3 and RCJ4 strains investigated in this study as components of a bacterial consortium. The remaining authors declare no competing interests.

Author contribution

M. de la L. Mora (MLM) acquired funding, conceived the study together with C. Jerez-Quezada (CJQ) and M. Abanto (MA), contributed to the experimental design, and provided scientific supervision on LMWOAs and their dynamics within the soil–plant–microorganism system. CJQ, MA, and MLM developed the experimental design as part of CJQ's doctoral research. CJQ performed the experimental work, conducted the microbiological and molecular analyses, interpreted the data, performed the statistical analyses, prepared the figures, and wrote the original manuscript. MA supervised the microbiological and genomic analyses, contributed to data interpretation, and supervised the statistical analyses and figure preparation. P. Barra (PB) supervised primer design, gene expression analyses, and the interpretation of the molecular results. D. Menezes-Blackburn (DMB) supervised the experimental design and interpretation of the interactions between LMWOAs and P, including the physicochemical processes underlying P dynamics. All authors critically revised the manuscript, contributed to its intellectual content, and approved the final version.

Acknowledgements

This work was supported by FONDECYT Regular Project No. 1230084 (MLM), 1241293 (PJB) and 1251164 (MA). Anillos de Investigación en Áreas Temáticas Específicas ATE250028 (PJB), and ANID Doctoral Scholarship N° 21241290 (CJ). We thank the Scientific and Technological Bioresource Nucleus (BIOREN) and the Biocontrol Research Laboratory for providing resources, infrastructure, and laboratory space.

Data availability statement

The genome sequences generated during this study have been deposited in GenBank under BioProject PRJNA1480829, with accession numbers JBZYXO000000000, JBZYXP000000000, and JBZYXQ000000000. The bacterial strains used in this study have been deposited in public culture collections under accession numbers RGM 3283 and RGM 3284 at the Chilean Collection of Microbial Genetic Resources (CChRGM, Instituto de Investigaciones Agropecuarias, INIA, Chillán, Chile) and CCCT 26.14 at the Chilean Type Culture Collection (CCCT, Scientific and Technological Bioresource Nucleus BIOREN, Universidad de La Frontera, Temuco, Chile). Additional datasets generated and analyzed during the current study are available from the corresponding author upon reasonable request.

References

1. Al-Kalbani A, Menezes-Blackburn D, Waladwadi J, Al-Ismaily S, Al-Siyabi B (2025) NaCl-induced soil stress regulates the diversity of soil bacteria and their ability to metabolize low molecular weight organic acids. J Saudi Soc Agricultural Sci 24(4):30. https://doi.org/10.1007/s44447-025-00036-5
2. Arifin M, Devnita R, Anda M, Goenadi DH, Nugraha A (2022) Characteristics of Andisols Developed from Andesitic and Basaltic Volcanic Ash in Different Agro-Climatic Zones. Soil Syst 6(4):78. https://doi.org/10.3390/soilsystems6040078

3. Assuero SG, Mollier A, Pellerin S (2004) The decrease in growth of phosphorus-deficient maize leaves is related to a lower cell production. Plant Cell Environ 27(7):887–895. https://doi.org/10.1111/j.1365-3040.2004.01194.x
4. Barra PJ, Duran P, Delgado M, Viscardi S, Claverol S, Larama G, Dumont M, de la Mora M L (2023) Proteomic response to phosphorus deficiency and aluminum stress of three aluminum-tolerant phosphobacteria isolated from acidic soils. IScience 26(10):107910. https://doi.org/10.1016/j.isci.2023.107910
5. Barra PJ, Parra-Almuna L, Pontigo S, Paredes C, Larama G, Valdebenito D, Jerez-Quezada C, Menezes-Blackburn D, de la Mora M L (2026) Phosphorus source shapes rhizosphere microbiome assembly and plant oxidative stress regulation in a volcanic Andisol: a path-analysis approach. Plant Physiol Biochem 238:111618. https://doi.org/10.1016/j.plaphy.2026.111618
6. Barra PJ, Pontigo S, Delgado M, Parra–Almuna L, Duran P, Valentine AJ, Jorquera MA, de la Mora M L (2019) Phosphobacteria inoculation enhances the benefit of P–fertilization on Lolium perenne in soils contrasting in P–availability. Soil Biol Biochem 136:107516. https://doi.org/10.1016/j.soilbio.2019.06.012
7. Barra PJ, Viscardi S, Jorquera MA, Duran PA, Valentine AJ, de la Mora L (2018) M. Understanding the Strategies to Overcome Phosphorus–Deficiency and Aluminum–Toxicity by Ryegrass Endophytic and Rhizosphere Phosphobacteria. *Frontiers in Microbiology*, *9*. https://doi.org/10.3389/fmicb.2018.01155
8. Bergkemper F, Schöler A, Engel M, Lang F, Krüger J, Schloter M, Schulz S (2016) Phosphorus depletion in forest soils shapes bacterial communities towards phosphorus recycling systems. Environ Microbiol 18(6):1988–2000. https://doi.org/10.1111/1462-2920.13188
9. Blazanin M (2023) *gcplyr: an R package for microbial growth curve data analysis*. https://doi.org/10.1101/2023.04.30.538883
10. Boden JS, Zhong J, Anderson RE, Stüeken EE (2024) Timing the evolution of phosphorus-cycling enzymes through geological time using phylogenomics. Nat Commun 15(1):3703. https://doi.org/10.1038/s41467-024-47914-0
11. Bruna P, Barra PJ, García M, Liachko I, de la Luz Mora M, Dutilh BE, Abanto M (2026) Unraveling plasmid contributions to phosphorus acquisition in soil microbiomes. Environ Microbiome 21(1):69. https://doi.org/10.1186/s40793-026-00887-7
12. Cortés-Albayay C, Delgado-Torres M, Larama G, Paredes-Negron C, de la Luz Mora M, Durán P, Barra PJ (2024) Comparative genomics of plant growth promoting phosphobacteria isolated from acidic soils. Antonie Van Leeuwenhoek 117(1):76. https://doi.org/10.1007/s10482-024-01961-1
13. Dabare S, Munaweera I, Diyabalanage S (2026) Sustainable mechanochemical activation of rock phosphate with oxalic acid for high-efficiency phosphorus fertilizers. RSC Adv 16(16):14135–14158. https://doi.org/10.1039/D5RA09011C
14. Dai Z, Liu G, Chen H, Chen C, Wang J, Ai S, Wei D, Li D, Ma B, Tang C, Brookes PC, Xu J (2020) Long-term nutrient inputs shift soil microbial functional profiles of phosphorus cycling in diverse agroecosystems. ISME J 14(3):757–770. https://doi.org/10.1038/s41396-019-0567-9
15. de Almeida Leite R, Martins da Costa E, Michel C, Amaral Leite D, de Oliveira-Longatti A, de Lima SM, Konstantinidis W, K. T., de Souza Moreira FM (2024) Genomic insights into organic acid production and plant growth promotion by different species of phosphate-solubilizing bacteria. *World Journal of Microbiology and Biotechnology*, *40*(10), 311. https://doi.org/10.1007/s11274-024-04119-3
16. De Coster W, D'Hert S, Schultz DT, Cruts M, Van Broeckhoven C (2018) NanoPack: visualizing and processing long-read sequencing data. Bioinformatics 34(15):2666–2669. https://doi.org/10.1093/bioinformatics/bty149
17. De Ferrari FN, Jofré-Fernández I, Matus F, Aburto F, Kerman J, Rojas C, Merino-Guzmán C (2026) A disturbance in the aggregates: wildfire reorganizes microbial substrate use across contrasting climatic windows in volcanic soils of native and managed forests. Biol Fertil Soils. https://doi.org/10.1007/s00374-026-02036-1
18. FAO (2008) *Efficiency of soil and fertilizer phosphorus use* (J. K. A. E. Syers, A. E. Johnston, & D. Curtin, Eds.; 1st ed., Vol. 1)
19. Hirshfield IN, Terzulli S, O'Byrne C (2003) Weak Organic Acids: A Panoply of Effects on Bacteria. Sci Prog 86(4):245–270. https://doi.org/10.3184/003685003783238626
20. Ji Q-Y, Wang W, Yan H, Qu H, Liu Y, Qian Y, Gu R (2023) The Effect of Different Organic Acids and Their Combination on the Cell Barrier and Biofilm of Escherichia coli. Foods 12(16):3011. https://doi.org/10.3390/foods12163011
21. Johan PD, Ahmed OH, Omar L, Hasbullah NA (2021) Phosphorus Transformation in Soils Following Co-Application of Charcoal and Wood Ash. *Agronomy*, *11*(10), 2010. https://doi.org/10.3390/agronomy11102010
22. Kalayu G (2019) Phosphate Solubilizing Microorganisms: Promising Approach as Biofertilizers. *International Journal of Agronomy*, *2019*, 1–7. https://doi.org/10.1155/2019/4917256
23. Kanehisa M (2002) *The KEGG Database* (pp. 91–103). https://doi.org/10.1002/0470857897.ch8
24. Karpiński TM, Ożarowski M (2024) Plant Organic Acids as Natural Inhibitors of Foodborne Pathogens. Appl Sci 14(14):6340. https://doi.org/10.3390/app14146340
25. Kolmogorov M, Yuan J, Lin Y, Pevzner PA (2019) Assembly of long, error-prone reads using repeat graphs. Nat Biotechnol 37(5):540–546. https://doi.org/10.1038/s41587-019-0072-8
26. Koul B, Yakoob M, Shah MP (2022) Agricultural waste management strategies for environmental sustainability. Environ Res 206:112285. https://doi.org/10.1016/j.envres.2021.112285
27. Kovanda L, Zhang W, Wei X, Luo J, Wu X, Atwill ER, Vaessen S, Li X, Liu Y (2019) In Vitro Antimicrobial Activities of Organic Acids and Their Derivatives on Several Species of Gram-Negative and Gram-Positive Bacteria. Molecules 24(20):3770. https://doi.org/10.3390/molecules24203770
28. Luo B, Liu F, Yang R, Li W, Xu A, Huang Q, Wu R, Yi Y, Zhong S, Qin F, Wei C (2025) Decoupling the effects of organic acid and EPS in phosphorus activation by phosphate solubilizing bacteria: From screening to morphological transformation analysis. Environ Technol Innov 40:104389. https://doi.org/10.1016/j.eti.2025.104389

29. Meier-Kolthoff JP, Göker M (2019) TYGS is an automated high-throughput platform for state-of-the-art genome-based taxonomy. Nat Commun 10(1):2182. https://doi.org/10.1038/s41467-019-10210-3
30. Menezes-Blackburn D, Bol R, Klumpp E, Missong A, Nischwitz V, Haygarth PM (2021) Citric Acid Effect on the Abundance, Size and Composition of Water-Dispersible Soil Colloids and Its Relationship to Soil Phosphorus Desorption: A Case Study. J Soil Sci Plant Nutr 21(3):2436–2446. https://doi.org/10.1007/s42729-021-00534-9
31. Menezes-Blackburn D, Paredes C, Zhang H, Giles CD, Darch T, Stutter M, George TS, Shand C, Lumsdon D, Cooper P, Wendler R, Brown L, Blackwell M, Wearing C, Haygarth PM (2016) Organic Acids Regulation of Chemical–Microbial Phosphorus Transformations in Soils. Environ Sci Technol 50(21):11521–11531. https://doi.org/10.1021/acs.est.6b03017
32. Merino-Guzmán C, Jofré-Fernández I, Rojas C, De Ferrari FN, Fajardo M, Aburto F, Rubilar R, Stehr A, Duarte E, Dorner J, Matus F (2026) A long time since fire: Land-use legacy modulates microbial functional recovery in volcanic Andisols under Nothofagus forests and Pinus radiata plantations. Agric Ecosyst Environ 411:110648. https://doi.org/10.1016/j.agee.2026.110648
33. Mingji X, Chongling Y, Jing Y, Lily W (2009) Impact of Phenanthrene on Organic Acids Secretion and Accumulation by Perennial Ryegrass, Lolium perenne L., Root. Bull Environ Contam Toxicol 83(1):75–80. https://doi.org/10.1007/s00128-009-9775-8
34. Mira P, Yeh P, Hall BG (2022) Estimating microbial population data from optical density. PLoS ONE 17(10):e0276040. https://doi.org/10.1371/journal.pone.0276040
35. Mora M, de la Demanet L, Acuña R, Viscardi JJ, Jorquera S, Rengel M, Z., Durán P (2017) Aluminum-tolerant bacteria improve the plant growth and phosphorus content in ryegrass grown in a volcanic soil amended with cattle dung manure. Appl Soil Ecol 115:19–26. https://doi.org/10.1016/j.apsoil.2017.03.013
36. Mora M, de la Rosas L, Ribera A, A., Rengel Z (2009) Differential tolerance to Mn toxicity in perennial ryegrass genotypes: involvement of antioxidative enzymes and root exudation of carboxylates. Plant Soil 320(1–2):79–89. https://doi.org/10.1007/s11104-008-9872-1
37. Moropana TJ, Rensburg ELJ, Van, Makulana L, Phasha NN (2026) Comparative Efficiency of Fungal Organic Acids and Pure Acids in Tricalcium Phosphate Solubilisation. Microorganisms 14(2):424. https://doi.org/10.3390/microorganisms14020424
38. Neculman R, Matus F, Godoy R, de la Mora M L., Rumpel C (2021) Carbon Mineralization Controls in Top- and Subsoil Horizons of Two Andisols Under Temperate Old-Growth Rain Forest. J Soil Sci Plant Nutr 21(1):780–790. https://doi.org/10.1007/s42729-020-00400-0
39. Negrón CP, Suazo-Hernández J, de la Mora M L., Duran P (2025) Lemon Peel Waste as a Natural Enhancer for Increasing Phosphorus Solubilization in Phosphate Rocks. J Soil Sci Plant Nutr 25(2):4796–4812. https://doi.org/10.1007/s42729-025-02429-5
40. ODEPA (2022) *Boletín de Empleo*. chrome-extension://efaidnbmnnnibpcajpcglclefindmkaj/https://bibliotecadigital.odepa.gob.cl/bitstream/handle/20.500.12650/71976/BEmpleo122022.pdf
41. ODEPA (2024) *Boletín regional de exportaciones silvoagropecuarias*. chrome-extension://efaidnbmnnnibpcajpcglclefindmkaj/https://bibliotecadigital.odepa.gob.cl/bitstream/handle/20.500.12650/73145/BRegionalExportacionesSi
42. Oliverio AM, Bissett A, McGuire K, Saltonstall K, Turner BL, Fierer N (2020) The Role of Phosphorus Limitation in Shaping Soil Bacterial Communities and Their Metabolic Capabilities. MBio 11(5). https://doi.org/10.1128/mBio.01718-20
43. Paredes C, Staunton S, Simeone GDR, Rao MA, Violante A, de la Mora L, M (2021) Citrus Residue Enhances the Effectiveness of Beef Cattle Manure Improving the Phosphorus Availability in Acidic Andisol. Commun Soil Sci Plant Anal 52(21):2767–2781. https://doi.org/10.1080/00103624.2021.1956522
44. Park Y, Solhtalab M, Thongsomboon W, Aristilde L (2022) Strategies of organic phosphorus recycling by soil bacteria: acquisition, metabolism, and regulation. Environ Microbiol Rep 14(1):3–24. https://doi.org/10.1111/1758-2229.13040
45. Parks DH, Imelfort M, Skennerton CT, Hugenholtz P, Tyson GW (2015) CheckM: assessing the quality of microbial genomes recovered from isolates, single cells, and metagenomes. Genome Res 25(7):1043–1055. https://doi.org/10.1101/gr.186072.114
46. Parra-Almuna L, Pontigo S, Ruiz A, González F, Ferrol N, de la Mora M L., Cartes P (2024) Dissecting the Roles of Phosphorus Use Efficiency, Organic Acid Anions, and Aluminum-Responsive Genes under Aluminum Toxicity and Phosphorus Deficiency in Ryegrass Plants. Plants 13(7):929. https://doi.org/10.3390/plants13070929
47. Pfaffl MW (2001) A new mathematical model for relative quantification in real-time RT-PCR. Nucleic Acids Res 29(9):45e–445. https://doi.org/10.1093/nar/29.9.e45
48. Poblete-Grant P, Cartes P, Pontigo S, Biron P, de La Mora L, M., Rumpel C (2022) Phosphorus fertiliser source determines the allocation of root-derived organic carbon to soil organic matter fractions. Soil Biol Biochem 167:108614. https://doi.org/10.1016/j.soilbio.2022.108614
49. Poblete-Grant P, Suazo-Hernández J, Condron L, Rumpel C, Demanet R, Malone SL, de Mora M L. L (2020) Soil available P, soil organic carbon and aggregation as affected by long-term poultry manure application to Andisols under pastures in Southern Chile. Geoderma Reg 21:e00271. https://doi.org/10.1016/j.geodrs.2020.e00271
50. Rodríguez R, Barra PJ, Larama G, Carrion VJ, de la Luz Mora M, Hale L, Durán P (2023) Microbiome engineering optimized by Antarctic microbiota to support a plant host under water deficit. *Frontiers in Plant Science*, *14*. https://doi.org/10.3389/fpls.2023.1241612
51. Rosas A, Rengel Z, Ribera A, de La Mora L, M (2011) Phosphorus nutrition alleviates manganese toxicity in Lolium perenne and Trifolium repens. J Plant Nutr Soil Sci 174(2):210–219. https://doi.org/10.1002/jpln.201000104
52. Santos-Beneit F (2015) The Pho regulon: a huge regulatory network in bacteria. *Frontiers in Microbiology*, *6*. https://doi.org/10.3389/fmicb.2015.00402
53. Saxena J, Rawat J, Sanwal P (2016) Enhancement of Growth and Yield of *Glycine max* Plants with Inoculation of Phosphate Solubilizing Fungus *Aspergillus niger* K7 and Biochar Amendment in Soil. Commun Soil Sci Plant Anal 47(20):2334–2347. https://doi.org/10.1080/00103624.2016.1243708

54. Schwengers O, Jelonek L, Dieckmann MA, Beyvers S, Blom J, Goesmann A (2021) Bakta: rapid and standardized annotation of bacterial genomes via alignment-free sequence identification. Microb Genomics 7(11). https://doi.org/10.1099/mgen.0.000685
55. Siles JA, Starke R, Martinovic T, Parente Fernandes ML, Orgiazzi A, Bastida F (2022) Distribution of phosphorus cycling genes across land uses and microbial taxonomic groups based on metagenome and genome mining. Soil Biol Biochem 174:108826. https://doi.org/10.1016/j.soilbio.2022.108826
56. Suzuki MT, Taylor LT, DeLong EF (2000) Quantitative Analysis of Small-Subunit rRNA Genes in Mixed Microbial Populations via 5'-Nuclease Assays. Appl Environ Microbiol 66(11):4605–4614. https://doi.org/10.1128/AEM.66.11.4605-4614.2000
57. Wang Y, Gao M, Wang Z, Huang T, Li H (2023) How Organic Acids Affect Plant Nitrogen and Phosphorus Uptake Under Different Fertilization Treatments. J Soil Sci Plant Nutr 23(4):6048–6058. https://doi.org/10.1007/s42729-023-01463-5
58. Wang Y, Luo D, Xiong Z, Wang Z, Gao M (2023) Changes in rhizosphere phosphorus fractions and phosphate-mineralizing microbial populations in acid soil as influenced by organic acid exudation. Soil Tillage Res 225:105543. https://doi.org/10.1016/j.still.2022.105543
59. Wei Y, Zhao Y, Shi M, Cao Z, Lu Q, Yang T, Fan Y, Wei Z (2018) Effect of organic acids production and bacterial community on the possible mechanism of phosphorus solubilization during composting with enriched phosphate-solubilizing bacteria inoculation. Bioresour Technol 247:190–199. https://doi.org/10.1016/j.biortech.2017.09.092
60. Wiesenbauer J, Gorka S, Jenab K, Schuster R, Kumar N, Rottensteiner C, König A, Kraemer S, Inselsbacher E, Kaiser C (2025) Preferential use of organic acids over sugars by soil microbes in simulated root exudation. Soil Biol Biochem 203:109738. https://doi.org/10.1016/j.soilbio.2025.109738
61. Xiong C, Guo Z, Chen SS, Gao Q, Kishe MA, Shen Q (2020) Understanding the pathway of phosphorus metabolism in urban household consumption system: A case study of Dar es Salaam, Tanzania. J Clean Prod 274:122874. https://doi.org/10.1016/j.jclepro.2020.122874
62. Yang L, Wu P, Yang W, Chen Y, Jing H (2026) Soil Humic Substances and Root Exudates: Key Factors Modulating Cadmium Mobility in Paddy Soils Under Organic Fertilization. Land Degrad Dev. https://doi.org/10.1002/ldr.70850
63. Zhang J, Gao L, Pang Z, Liu L, Chen X, Wang S, Wang H, Tong R, Shi C, Chen X (2021) Effect of low-molecular-weight organic acids on phosphorus soil activation: A laboratory study of the soils from Wangbeng section of the Huaihe River Basin, China. Plant Soil Environ 67(11):660–667. https://doi.org/10.17221/379/2021-PSE
64. Zheng J, Shi G, Dini-Andreote F, Yang Y, Jiang Y (2026) Root-derived low molecular weight organic acids modulate keystone microbial taxa impacting plant phosphorus acquisition. J Adv Res 81:95–109. https://doi.org/10.1016/j.jare.2025.06.032
65. Zhi L, Zheng B, Xu Y, Xu J, Peñuelas J, Sardans J, Chang Y, Jin S, Ying H, Ding K (2025) Organic fertilizers shape the bacterial communities harboring pqqC and phoD genes by altering organic acids, leading to improved phosphorus utilization. Soil Ecol Lett 7(2):250296. https://doi.org/10.1007/s42832-025-0296-0

Figures

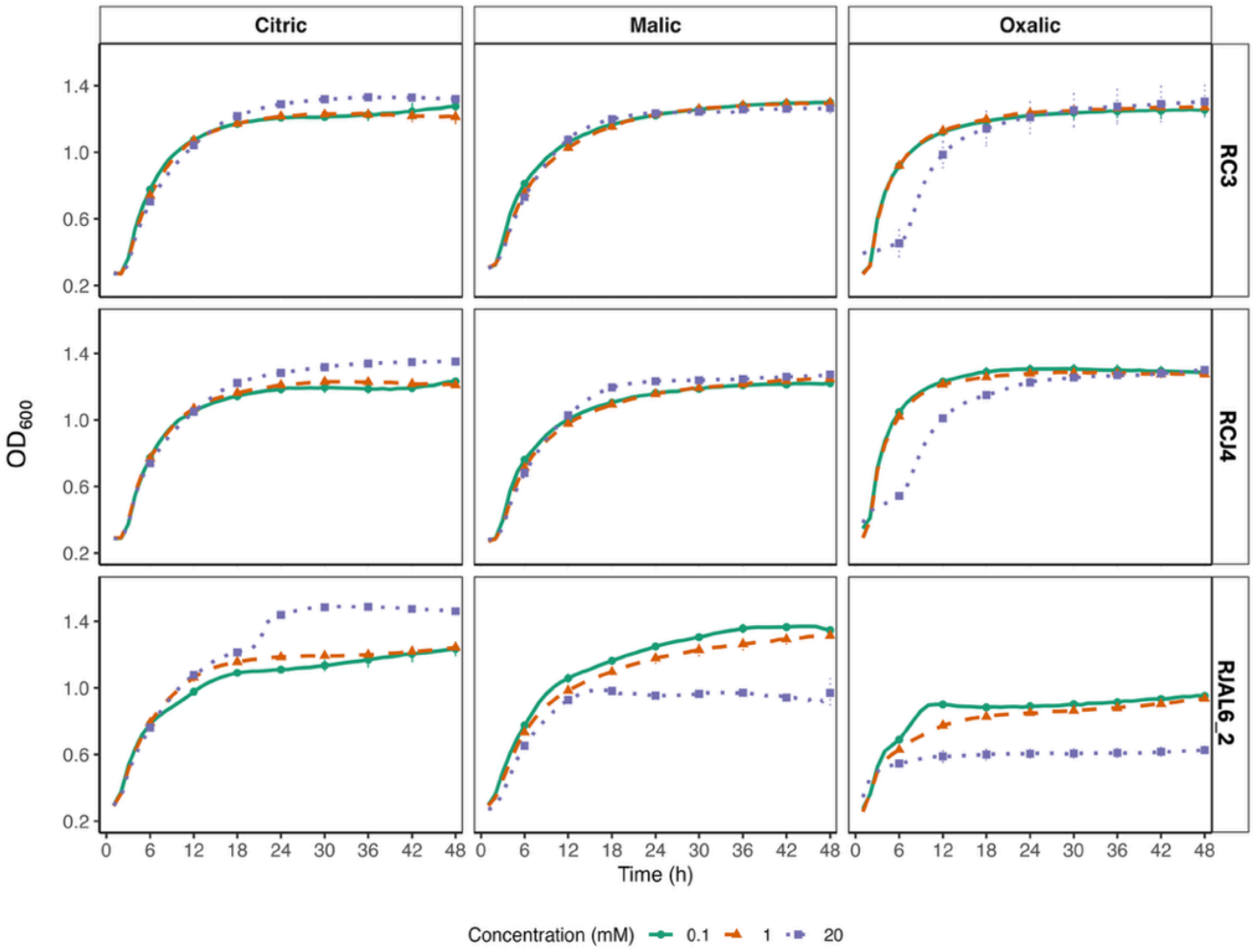


Figure 1

Growth curves of A) *K. michiganensis* RC3, B) *K. michiganensis* RCJ4 and C) *E. ludwigii* RJAL6_2, grown in minimal medium containing malic, citric, and oxalic acid in different concentrations, under less soluble phosphorus (P−). Bacterial growth was monitored by measuring optical density at 600 nm (OD_{600})

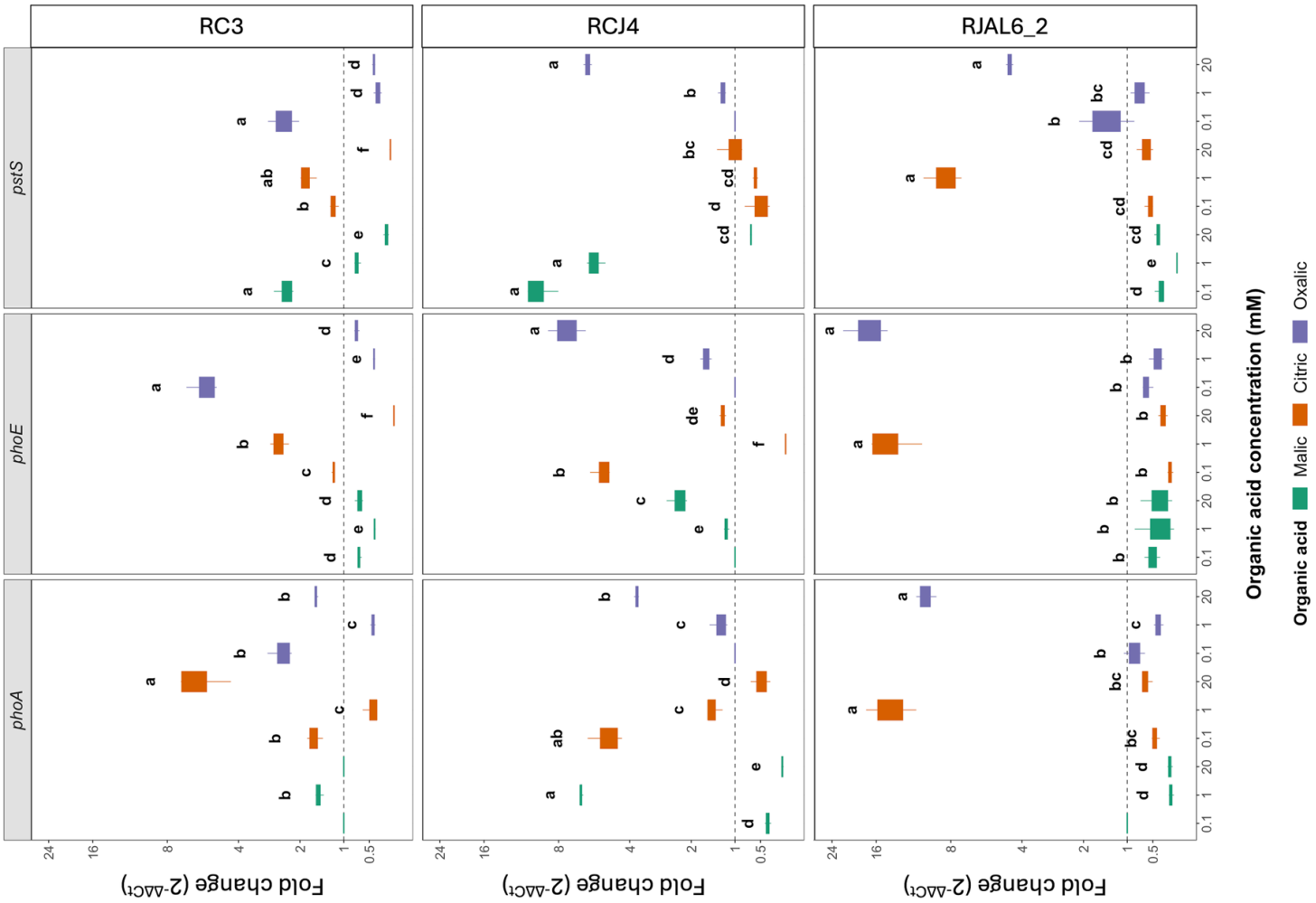


Figure 2

Boxplots showing the relative expression ($2^{-\Delta\Delta Ct}$) of the *phoA*, *phoE,* and *pstS* genes in *K. michiganensis* RC3, RCJ4 and *E. ludwigii* RJAL6_2 following exposure to citric, malic, and oxalic acids under poor phosphorus availability (P−). Different lowercase letters indicate significant differences among organic acid × concentration treatment combinations, based on estimated marginal means (emmeans) from a two-way ANOVA followed by Tukey-adjusted pairwise comparisons ($p < 0.05$).

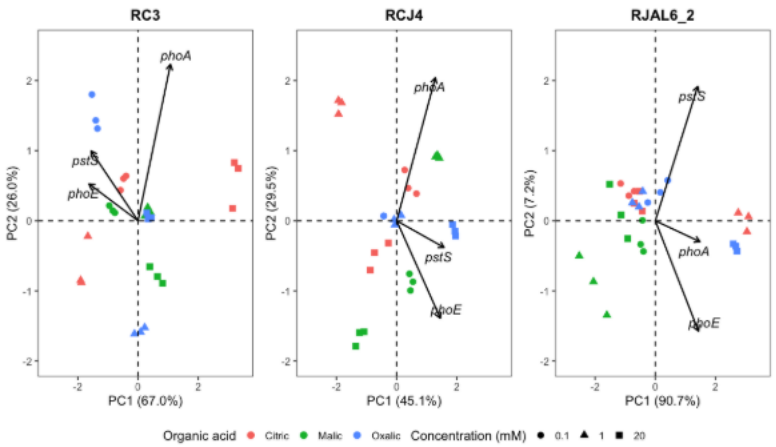


Figure 3

Principal component analysis (PCA) of P acquisition gene expression in phosphate-solubilizing bacteria exposed to different organic acids and concentrations. PCA was performed separately for *K. michiganensis*RC3, *K. michiganensis* RCJ4, and *Enterobacter ludwigii* RJAL6_2. Colors indicate the organic acid treatment (citric, malic, or oxalic acid), while point shapes represent organic acid concentrations (0.1, 1, and 20 mM). Arrows represent the

contribution and direction of individual P acquisition genes (*phoA*, *phoE*, and *pstS*) to the principal components. Percentages shown on the axes indicate the proportion of total variance explained by each principal component.

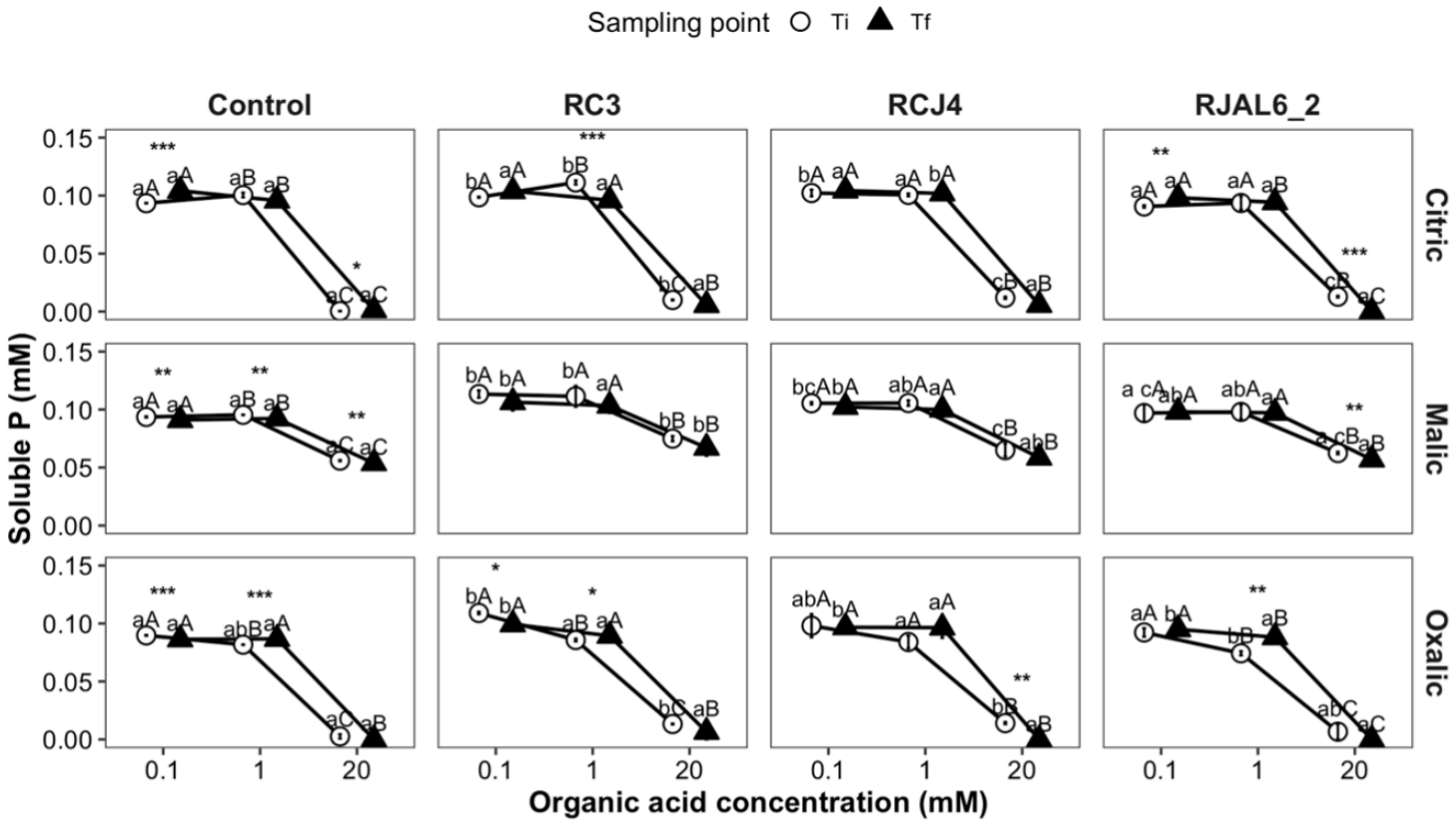


Figure 4

Soluble phosphorus concentration determined by Murphy and Riley methodology in culture media supplemented with different organic acids and concentrations after incubation with P-solubilizing bacteria. Data are presented as mean ± standard deviation. Different lowercase letters indicate significant differences among treatments (Control, RC3, RCJ4, and RJAL6_2) within each organic acid, concentration, and sampling time, whereas different uppercase letters indicate significant differences among organic acid concentrations within each treatment, organic acid, and sampling time (one-way ANOVA followed by Tukey's HSD post hoc test, $p < 0.05$). Asterisks indicate significant differences between the initial (Ti) and final (Tf) sampling times for each treatment, organic acid, and concentration, as determined by Student's t-test ($p < 0.05$, $p < 0.01$, $p < 0.001$).

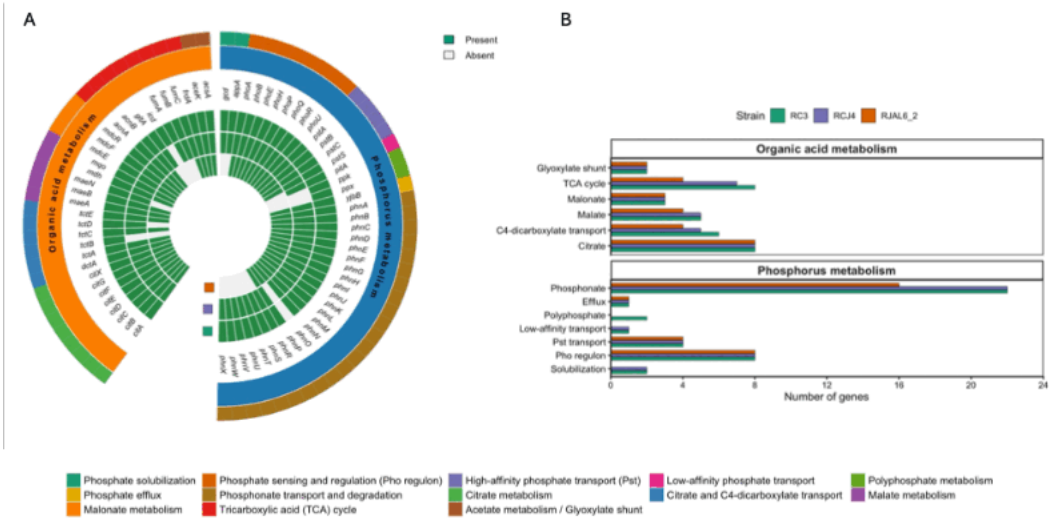


Figure 5

Comparative genomic distribution of genes involved in phosphorus and organic acid metabolism in three phosphate-solubilizing bacterial isolates. (A) Circular presence–absence plot of genes identified by KEGG and EggNOG genome annotation. Genes were grouped according to their predicted functional categories related to phosphorus metabolism and organic acid metabolism. (B) Horizontal grouped bar plots showing the number of annotated genes in each functional category for each isolate.

Supplementary Files

This is a list of supplementary files associated with this preprint. Click to download.

- floatimage1.png
- Supplementaryfigures.pdf